Continental Shelf Research, Vol. 9, No. 12, pp. 1071–1083, 1989.
Printed in Great Britain.

0278-4343/89 $3.00 + 0.00
Pergamon Press plc.

Volume transport in the Alaska Coastal Current

JAMES D. SCHUMACHER,* PHYLLIS J. STABENO* and ANDREW T. ROACH*

(Received 9 March 1989; accepted 20 April 1989)

Abstract—Nine moorings were deployed in three sections in the Shelikof Strait/Semidi Islands region of the Alaskan continental shelf during the period of August 1984 to July 1985. Analysis of the resulting current and bottom pressure data, together with surface wind, provides a new understanding of transport in the Alaska Coastal Current. Using current observations, mean volume transport through the Shelikof sea valley was computed to be 0.85×10^6 m^3 s^{-1}, which is in good agreement with estimates of transport obtained from hydrographic data. Approximately 75% of this flux flowed seaward through the Shelikof sea valley, with the remainder flowing along the Alaska Peninsula. Data showed the expected increase of volume transport concomitant with maximum freshwater discharge in autumn. The greatest monthly mean transport, however, occurred in winter and was related to wind forcing. On time intervals of days, fluctuations in transport were often large (up to 3.0×10^6 m^3 s^{-1}), and generally geostrophic ($r = 0.79$). Some of these fluctuations resulted from convergence of flow caused by the complex interaction of storms with orography. Approximately half of the fluctuations in volume transport were accounted for by the alongshore wind.

INTRODUCTION

DURING the past decade, knowledge of the physical oceanography of the Gulf of Alaska has grown substantially. Discovery of the Alaska Coastal Current (ACC), a narrow coastal jet extending more than 1000 km along the coast (Fig. 1), was one of the most important advances. This is a vigorous coastal current with speeds as large as 175 cm s^{-1}. Transport is driven by the large flux of freshwater along the coast of Alaska (ROYER, 1982). The alongshore wind perturbs this flow through both confinement of the freshwater and alteration of coastal sea level (SCHUMACHER and REED, 1980; ROYER, 1981; REED and SCHUMACHER, 1981). Between Kodiak Island and the mainland, differential Ekman pumping generates fluctuations in transport (REED and SCHUMACHER, 1989). The maximum freshwater input is in autumn (ROYER, 1982). Concomitantly, speeds in the ACC increase markedly and volume transport is 2–3 times as great as observed during summer, often exceeding 1.9×10^6 m^3 s^{-1}. After leaving the northeastern coast of Alaska, most of the ACC flows through Shelikof Strait, with a portion continuing westward to Unimak Pass (SCHUMACHER and REED, 1986). To date, all transport estimates have been based on hydrographic data which are sensitive to the selection of a level of no motion.

In this paper, we present the first estimates of transport in the ACC computed using current and bottom pressure records. These records were collected between August 1984 and July 1985 in the western Gulf of Alaska (Fig. 1). This experiment was part of

* Pacific Marine Environmental Laboratory, 7600 Sand Point Way NE, Seattle, WA 98115, U.S.A.

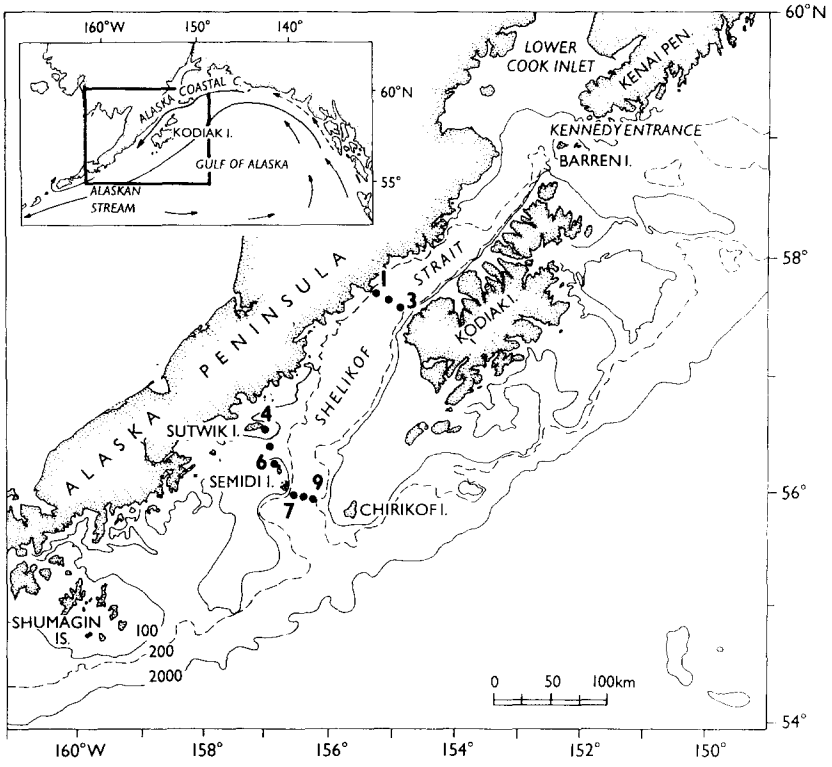

Fig. 1. Study area setting. Positions of the nine moorings (dots) are indicated. Mooring numbers are consecutive but only outer ones are labeled. Shown in the insert is the regional circulation. Depths are in meters.

Fisheries Oceanography Coordinated Investigations (FOCI), a continuing NOAA program. The goal of FOCI is to understand biological and physical processes influencing recruitment of pollock (*Theragra chalcogramma*) in Shelikof Strait, Alaska. The objective of the research component presented here was to answer basic questions regarding characteristics of transport, including: what fraction of the transport is through the sea valley along the Alaska peninsula, and can transport be monitored with bottom pressure observations?

A description of current and bottom pressure data obtained during this experiment, together with surface winds, is presented in ROACH *et al.* (1987). REED *et al.* (1987) present a comprehensive analysis of hydrographic data collected in March and July 1985. The focus of this paper is to describe transport, to examine mechanisms causing fluctuations, and to investigate geostrophy.

OBSERVATIONS

The observational program

During 1984 and 1985, 35 current meters and six pressure gauges (Aanderaa model RCM-4 and WLR-5 or TG-3) were deployed on nine taut-wire moorings in the western Gulf of Alaska (Fig. 1). The moorings were arranged in three sections; data was recorded

at section 1 (moorings 1, 2 and 3) for 5 months (August 1984 to January 1985) and at sections 2 (moorings 4, 5 and 6) and 3 (moorings 6, 7 and 8) for 11 months (August 1984 to July 1985). Current meter depths and locations are shown in Fig. 2. Some instruments measured temperature and conductivity which were used to estimate salinity. The six bottom pressure gauges were located one at each end of a section. All gauges were mounted in a well on the anchor to avoid the effects of mooring motion.

Surface winds were computed from 6-hourly atmospheric surface pressure supplied by the Fleet Numerical Oceanography Center. These are geotriptic winds (a balance of

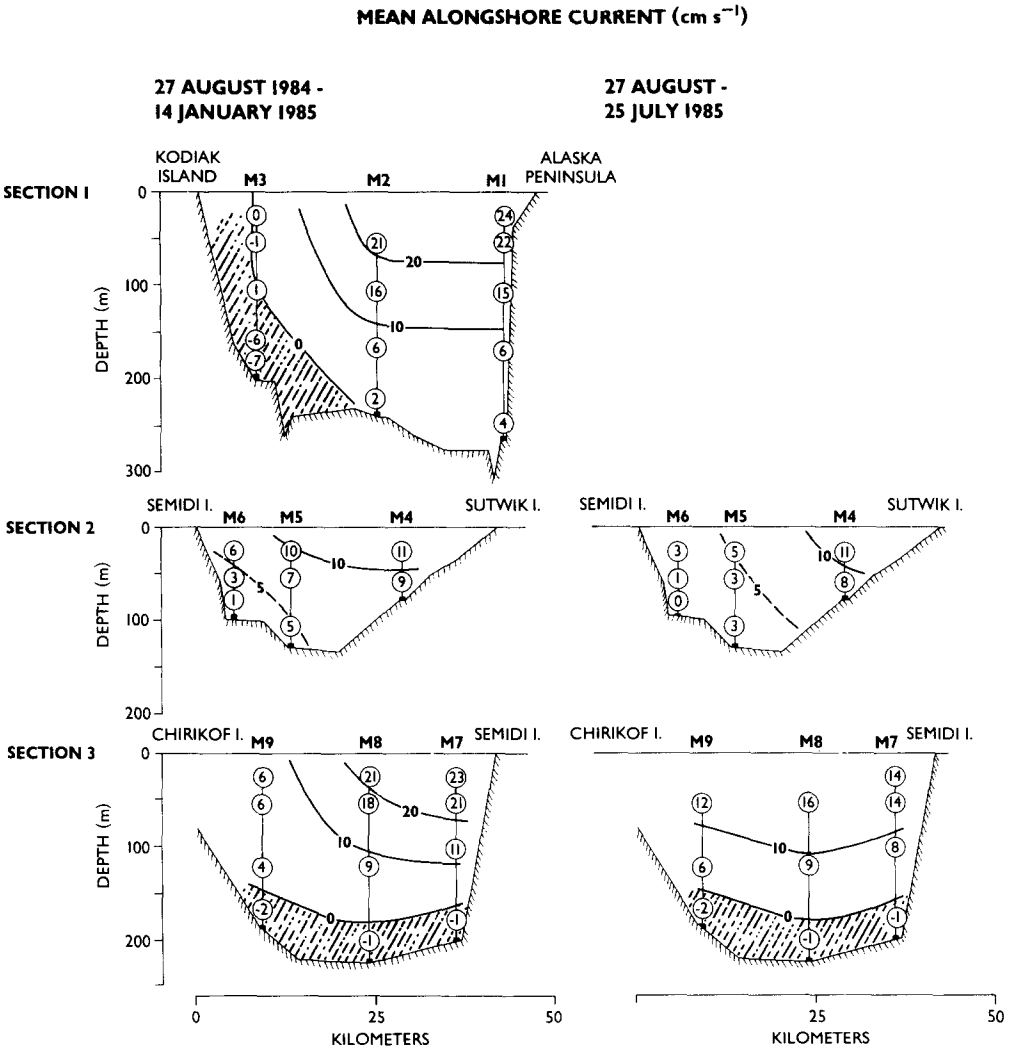

Fig. 2. Mean current velocity observed at section 1 (top), section 2 (middle) and section 3 (bottom). Contours of the alongshore (220°T, 250°T and 190°T for sections 1, 2 and 3, respectively) component of velocity are shown in the left column for the period 27 August 1984 to 14 January 1985, and in the right column for the period 27 August 1984 to 25 July 1985. Shaded areas represent inflow.

Coriolis, pressure gradient, centrifugal and friction forces) which were rotated 15° counterclockwise, reduced in speed by 30% from the geostrophic wind, and interpolated to the vicinity of Semidi Islands (Fig. 3).

The data

Since tides dominated the bottom pressure spectrum, the pressure records were detided prior to low-pass filtering and removing linear trends. The current and detided bottom pressure data were low-pass filtered with a cosine-squared tapered Lanczos filter and resampled at 6-hourly intervals. This filter passes more than 99% of the amplitude at periods greater than 44 h, 50% at 35 h and less than 0.5% at 25 h, effectively removing the tidal signal from the current records. Examples of low-pass filtered currents are shown in Fig. 3.

Estimates of transport were calculated from the current velocity components normal to each section, multiplied by estimates of cross-sectional area. These areas were computed as follows. Detailed bathymetry was compiled for each section using information from continuous depth recordings, soundings at CTD stations and standard charts. Between moorings, the midpoint was used to define the horizontal extent assigned a given current velocity. The horizontal length between a mooring and the edge of a section varied. At section 1, current was assumed to occur only seaward of mooring 1 and to extend from mooring 3 to Kodiak Island. At section 2, the current was assumed to extend halfway between the outer two moorings and the adjacent land. At section 3, the current was taken to extend halfway between mooring 7 and Semidi Island but only one-third of the way (a depth of 100 m) to Chirikof Island. The vertical length at each mooring was selected as the midpoint between adjacent current meters. For example, the velocity from instruments at a nominal depth of 26 m (the next current meter was at 56 m) was assigned to the upper 41 m of the water column. We assumed no shear in current velocity within a transport layer. Velocity was set at zero approximately 5 m above the bottom. All results presented here are based on 6-hourly time series.

Mean and low-frequency transport. The structure of the mean alongshore current shows the local manifestation of the ACC. During the period August to January (Fig. 2, left column), the ACC was strongest (>20 cm s^{-1}) in the upper 150 m on the northwest or west side of the sea valley at sections 1 and 3. The portion of the ACC which continued along the Peninsula (section 2), rather than following the sea valley (section 3), showed more moderate (~10 cm s^{-1}) flow. Inflow occurred in both sea valley sections (1 and 3). When averages over the entire observation period (August 1984 to July 1985: Fig. 2, right column) are considered, the flow pattern at section 3 is changed substantially from the August to January mean. Maximum velocities were smaller and more evenly distributed across the sea valley, although inflow remained on the bottom. This inflow supports conclusions from hydrographic data that an "estuarine-like" or two-layered flow exits (REED *et al.*, 1987) and emphasizes the care required in selecting a level of no motion for baroclinic calculations (REED and SCHUMACHER, 1989).

From August 1984 to January 1985 the mean and r.m.s. error of the volume flux through section 1 ($\bar{T}_1$) was $0.81 \pm 0.13 \times 10^6$ m^3 s^{-1} and the sum of the transport through the other two sections was 0.26 ± 0.04 ($\bar{T}_2$) + 0.68 ± 0.11 ($\bar{T}_3$) = $0.94 \pm 0.13 \times 10^6$ m^3 s^{-1} ($\bar{T}_{2+3}$). During this interval, transport balanced to within 15%. For the longer time interval (August 1984 to July 1985), mean volume transport in the ACC was calculated to be 0.19 ± 0.02 ($\bar{T}_2$) + 0.66 ± 0.08 ($\bar{T}_3$) = $0.85 \pm 0.10 \times 10^6$ m^3 s^{-1} ($\bar{T}_{2+3}$).

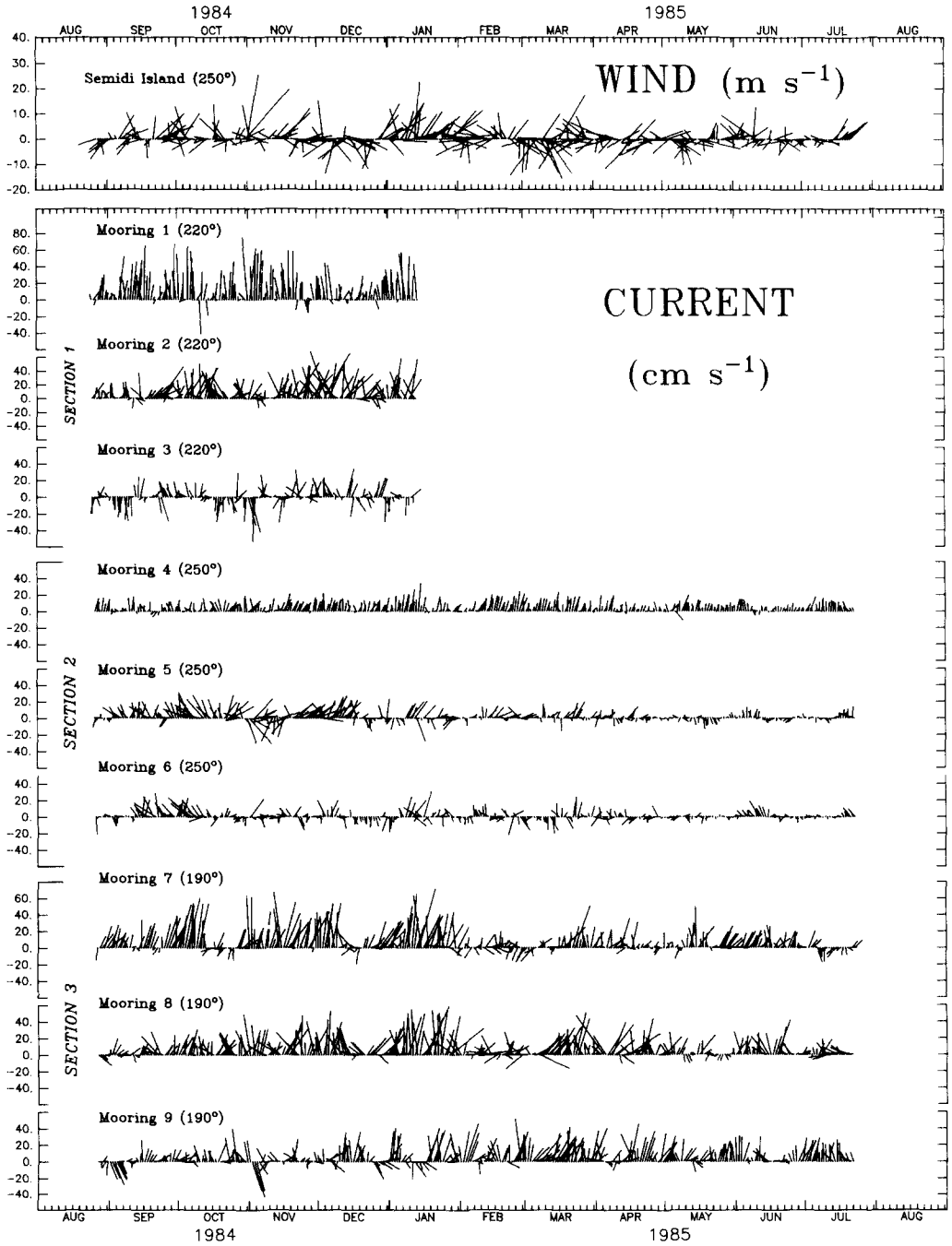

Fig. 3. Current time series from a nominal depth of 56 m. The daily vectors are shown relative to the axis of each section (given in parentheses).

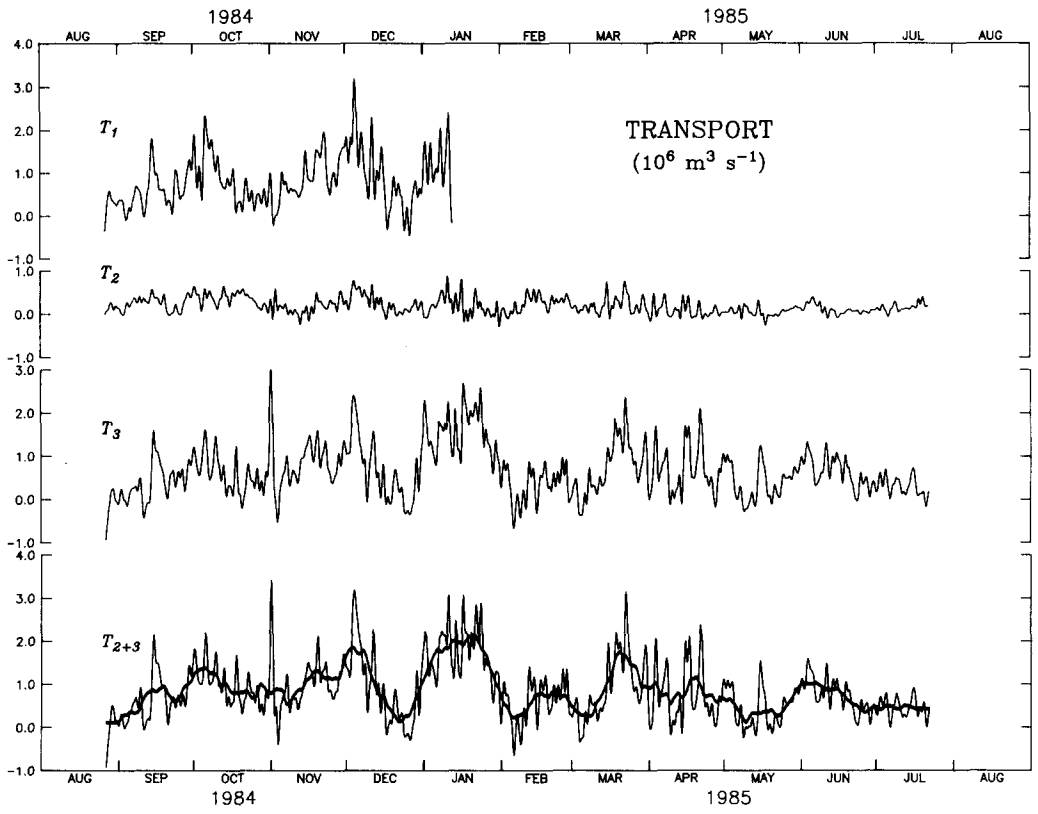

Fig. 4. Time series of transport through sections 1, 2, 3 and the sum of $T_2 + T_3$. (The heavy line is a 10-day running mean.)

Time series of transport through each of the three sections and T_{2+3} are shown in Fig. 4. The time series T_{2+3} was formed by adding the 6-hourly low-pass filtered transport data from sections 2 and 3; statistics were computed from this new series. All series had high frequency (0.2–0.5 cpd) fluctuations which became less prominent after May. These fluctuations were superimposed on a very low frequency signal (~0.03 cpd) which also decreased in amplitude in spring. There were four identifiable events in T_{2+3} (Fig. 4, Table 1), each lasting more than 10 days, during which transport exceeded the mean (0.85×10^6 m^3 s^{-1}). To help visualize these events, we applied a 10-day running mean to the transport series T_{2+3}. The average duration of these events was 23 days with a standard deviation of 11 days. During these pulses, the average transport was 1.49×10^6 m^3 s^{-1}. The event with maximum transport occurred during January.

Although the transport time series are rich in variability, spectral analysis showed no significant peaks (at the 95% significance level). For each series at least 66% of the variance occurred at periods longer than 10 days. The baroclinic instability identified in previous current data from Shelikof Strait was thought to be the source of most of the low-frequency current fluctuations (MYSAK *et al.*, 1981). This signal is clear in the current record from mooring 2 where the current vectors rotate back and forth across the section. Similar motion appears to a lesser degree at mooring 8. Analysis of current spectra,

Table 1. Statistics of very low frequency events in the 6-hourly total (T_{2+3}) transport time series. R.M.S. error estimates were calculated from the quotient of the standard deviation divided by the square root of the ratio of the record length divided by the integral time scale

Event no.	Observation period	Duration (days)	Volume transport ± r.m.s. error (10^6 m^3 s^{-1})
1	29 September, 0600 15 October, 0000	15.75	1.29 ± 0.12
2	14 November, 1200 15 December, 0600	31.0	1.39 ± 0.16
3	29 December, 1800 31 January, 0600	33.75	1.71 ± 0.15
4	14 March, 1800 27 March, 0600	12.75	1.56 ± 0.20

Table 2. Correlations at the 95% level between transport through section 1 (T_1), section 2 (T_2), section 3 (T_3), and section 2 + section 3 (T_{2+3})

	Variance (%)		
Transport	T_1	T_2	T_3
T_1	100		
T_2	22	100	
T_3	51	–	100
T_{2+3}	58	25	92

Numbers give the percent variance ($r^2 \times 100$) in each row which is explained by the column. Dashes indicates no significant correlation.

however, indicate that only at mooring 2 was the spectral peak statistically significant (Roach *et al.*, 1987). In the time series of volume transport, baroclinic instability was not a mechanism generating significant variability.

Relationships between transport time series. Fluctuations in transport through sections 2 and 3 were best correlated with those upstream through section 1 and were not significantly correlated with each other (Table 2). Fluct ations in T_1 accounted for over half of those in T_{2+3}. For all pairs, most of the coherent signal was in the longest period band (>19 days). Transports through sections 2 and 3 were coherent in only one frequency band (4.6–5.1 days) and this accounted for less than 6% of the total variance.

DISCUSSION

Forcing mechanisms

The primary cause of the annual variation in transport in the ACC is the freshwater runoff whose maximum occurs in autumn (Schumacher and Reed, 1980; Royer, 1981, 1982). The major source of this runoff is along the east and north coast of Alaska, before the ACC enters Shelikof Strait. Estimates of geostrophic transport based on CTD data from 20 occupations of seven stations along section 1 and collected between March 1985 and June 1988 yield a mean and standard deviation of 0.59 ± 0.32 × 10^6 m^3 s^{-1}. The reference levels used for geostrophic transport calculations vary across the section (Reed and Schumacher, 1989; Fig. 2). There were no CTD surveys during winter. The maximum of 1.18 × 10^6 m^3 s^{-1} occurred in October 1985. The mean and standard

deviation compares favorably with values estimated from current records: $\bar{T}_1 = 0.81 \pm 0.59 \times 10^6$ m^3 s^{-1}, or $\bar{T}_{2+3} = 0.85 \pm 0.68 \times 10^6$ m^3 s^{-1}.

There was also good agreement between calculated and observed transport over shorter time intervals. From 25 to 26 March 1985, CTD data were collected at stations along sections 2 and 3, providing estimates of 0.01×10^6 and 0.85×10^6 m^3 s^{-1}, respectively. (For the same time, current data were used to establish a 190-dbar level of no motion for section 3.) From current records the values were 0.05 and 0.86×10^6 m^3 s^{-1}, for sections 2 and 3, respectively.

Volume transport during October 1984 (Table 1) was enhanced by the maximum freshwater accumulation. Since there is no hydrographic data, we examine the current structure (Fig. 5) and salinity from moored instruments. During October, the largest current speeds and the greatest vertical shear occurred in the vicinity of moorings 6 and 7. This was accompanied by a marked increase in current speed and a decrease in salinity

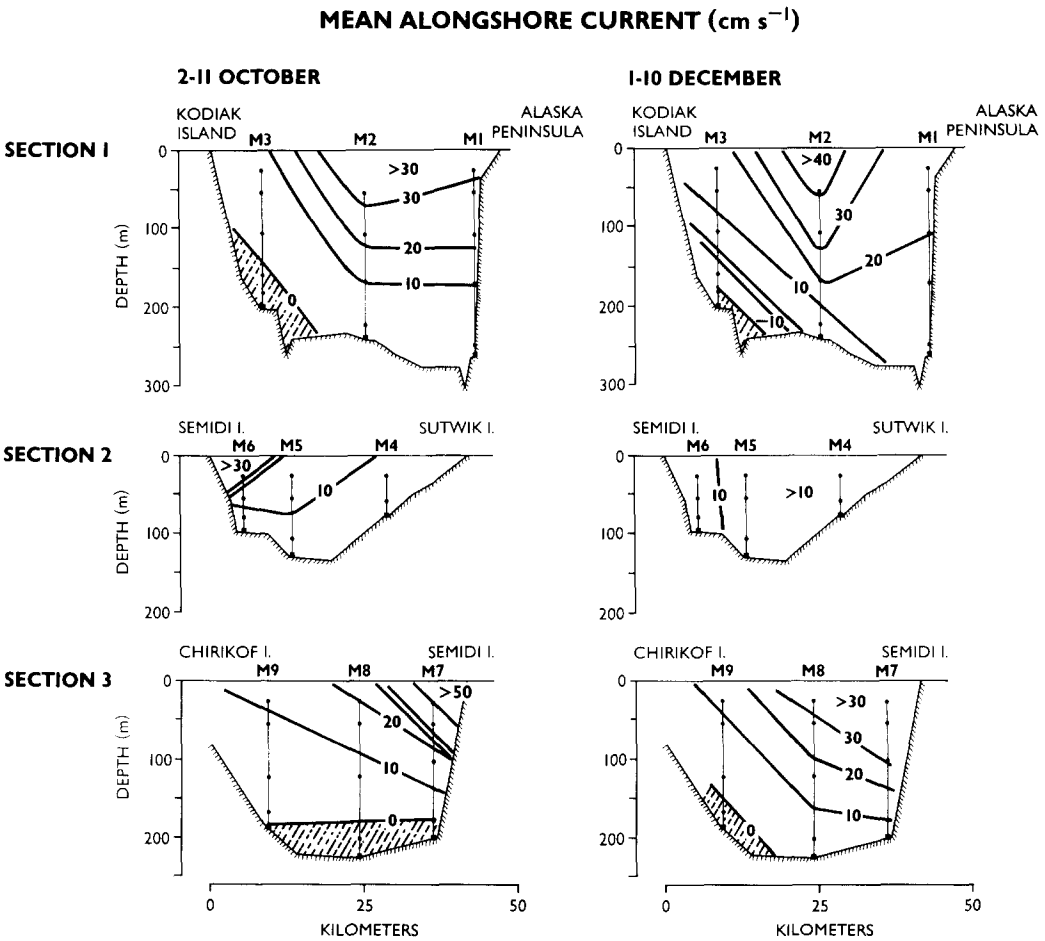

Fig. 5. Structure of the mean current for (a) 2–11 October and (b) 1–10 December 1984. Volume transport at section 1 was 1.4×10^6 (1.7×10^6), for section 2, 0.4×10^6 (0.5×10^6) and section 3, 1.0×10^6 (1.3×10^6) m^3 s^{-1} for the October (December) event.

of approximately 1 psu at moorings 4–7 in the upper 56 m of the water column. Both of these changes are consistent with observations made in autumn 1978 (SCHUMACHER and REED, 1986). We conclude that strong vertical shear and a narrow band of high speeds and marked decrease in salinity (as observed in October 1984) are features of the enhanced geostrophic transport associated with the large increase of freshwater which occurs during autumn.

Contrast these characteristics with those occurring during a transport pulse of similar magnitude that occurred in December (Fig. 5). At section 1 the higher current speeds occurred over a greater area than in October, with strong near-bottom flow toward the northeast compensating for increased southwestward flow. In section 2, the maximum current was near mooring 4 rather than at mooring 6, and both here and in section 3 vertical shear markedly decreased from values in October. Finally, there was no accompanying decrease in salinity at any mooring. The remaining three pulses had characteristics similar to those in December and represent fluctuations which were not directly related to the seasonally varying flux of freshwater.

Most of the remaining fluctuations were most likely caused by wind forcing. Early studies (SCHUMACHER and REED, 1980; ROYER, 1981; REED and SCHUMACHER, 1981) suggest that the alongshore component of the wind alters the cross-shelf distribution of mass and perturbs coastal sea level through Ekman transport. In the vicinity of Kodiak Island, complex wind patterns result from the interaction of storms with orography. Within the orographically bounded region of Shelikof Strait proper, nearshore isopycnal surfaces appear to be deepened through differential Ekman pumping (REED and SCHUMACHER, 1989). This causes large, rapid perturbations (about 0.4×10^6 m^3 s^{-1} in <3 days) in volume transport.

Because most of the sea valley is nearly parallel to and in close proximity of the coast, Ekman-driven coastal convergence should be important. Between September 1984 and January 1985, estimates of coherence (at the 95% level of significance) between the alongshore component (240°T) of the surface wind at Semidi Islands and water transport accounted for 39, 3 and 41% of the fluctuations in volume transport at sections 1, 2 and 3, respectively. For the series T_{2+3} approximately 45% (50% for the 11-month time interval) of the variance in transport could be explained by the alongshore wind.

Wind data collected from a research aircraft show convergence of geostropic and ageostrophic winds in the region between sections 1 and 2 (MACKLIN *et al.*, 1984). Under such meteorological conditions transport will be enhanced toward the southwest in Shelikof Strait. At the same time, over the open shelf west of Kodiak Island, onshore winds cause reduced transport out of the system. As a result sea level increases in the region bounded by the three sections. For example, between 30 October and 2 November 1984, an eastward-moving low pressure system passed within 250 km south of the study area. The distribution of surface atmospheric pressure (Fig. 6) caused onshore surface (geotriptic) winds over the open shelf and down-gradient (ageostrophic) winds in Shelikof Strait proper. Concomitant with the storm, near-surface currents at moorings 5–7 reversed and those at mooring 1 increased toward the southwest. As a result, transport through section 2 decreased markedly ($<0.02 \times 10^6$ m^3 s^{-1}), transport through section 3 was reduced and it increased through section 1. At all bottom pressure gauges the response was an increasing positive anomaly (>15 mbar), with a maximum occurring after about 36 h. As the storm moved eastward, wind forcing changed and the convergence of water transport ceased. As the dome of water relaxed, transport seaward

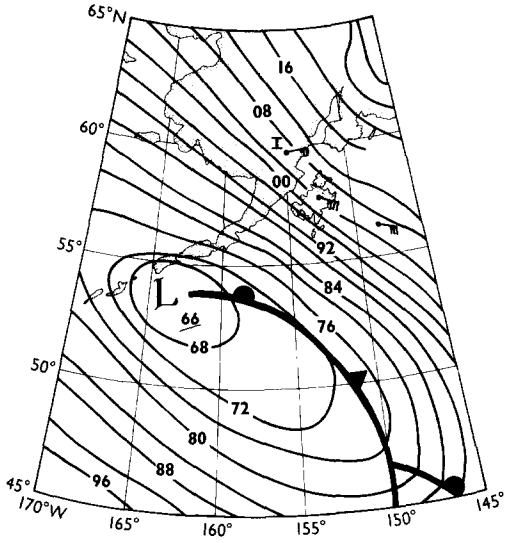

Fig. 6. Sea level atmospheric pressure for 1200 on 31 October 1984. The wind barbs are actual observations. Note how the barb at Iliamna (labeled I) indicates down-gradient winds similar to those in Shelikof Strait. Surface wind at Semidi Island was 12.5 m s^{-1} toward 300°T.

through section 3 increased by as much as 4.3 times greater than the mean. Volume transport then reversed at all locations as the system overshot equilibrium. The interaction is reversible. A high pressure system southwest of the Shelikof region generates offshore winds over the open shelf and northeastward winds in Shelikof Strait which result in divergent transport. The strong reversal of transport which occurred at the start of the time series in August is an example of such an event.

The integrated effect of storms also accounts for variations in volume transport over longer time intervals. Data on principal tracks of centers of cyclones at sea level (MARINER'S WEATHER LOG, 1985) provide necessary information to estimate the possible impact of storms. During January, five cyclones passed through the region bounded by 50°–55°N, and 155°–165°W, on trajectories from south to north. During February, only two storms passed through the southernmost portion of the area and they were on eastward trajectories. The difference in number and trajectory of these storms was reflected in the mean alongshore wind component (240°T) which reversed from 5.2 m s^{-1} in January to –0.2 m s^{-1} in February. Accompanying the difference in storm characteristics was a marked difference between the monthly transport in January (1.74×10^6 m^3 s^{-1}) and February (0.59×10^6 m^3 s^{-1}).

Geostrophy

One of the objectives of the field experiment was to determine if bottom pressure measurements could be used to calculate transport. Following BROWN *et al.* (1987), fluctuations in transport are related to bottom pressure via

$$G = (f\rho_o)^{-1} \int_{x_1}^{x_2} h(x) p_x dx, \tag{1}$$

where x is in the across-channel direction, G the geostrophic transport, p the bottom pressure, ρ_o mean density, f Coriolis and $h(x)$ depth. We have neglected the two terms

representing density anomalies, since the time series of salinity and temperature were not complete enough to calculate density. Bottom pressure records were limited to the endpoints of each section, so we assume that $h(x)$ = H, a constant. Deviation from this assumption was greatest at section 1 (30%) and least at section 3 (<10%). The correlations of transports with their associated pressure differences at sections 2 and 3 accounted for 50 and 62% of transport fluctuations, respectively. At section 1 there was no significant correlation. This was probably caused by two factors. The first is the deviation of $h(x)$ from constant value; the second is the strength of density anomalies which are largest at section 1 since it is nearer the freshwater sources.

For section 3, the geostrophic transport was calculated using equation (1) with ρ_o = 1 g cm^{-2}, $f = 1.23 \times 10^{-4}$ and H = 205 m. Shown in Fig. 7 are the demeaned and detrended transports, calculated from the velocity records (T_3) and the geostrophic relationship (G_3). The fluctuations calculated using equation (1) were nearly of the same magnitude as those observed; a least squares fit of $T_3 = \alpha\, G_3 + e$ yields $\alpha = 0.94$. The balance held for many of the strong pulses, at both short and long periods and for both in-

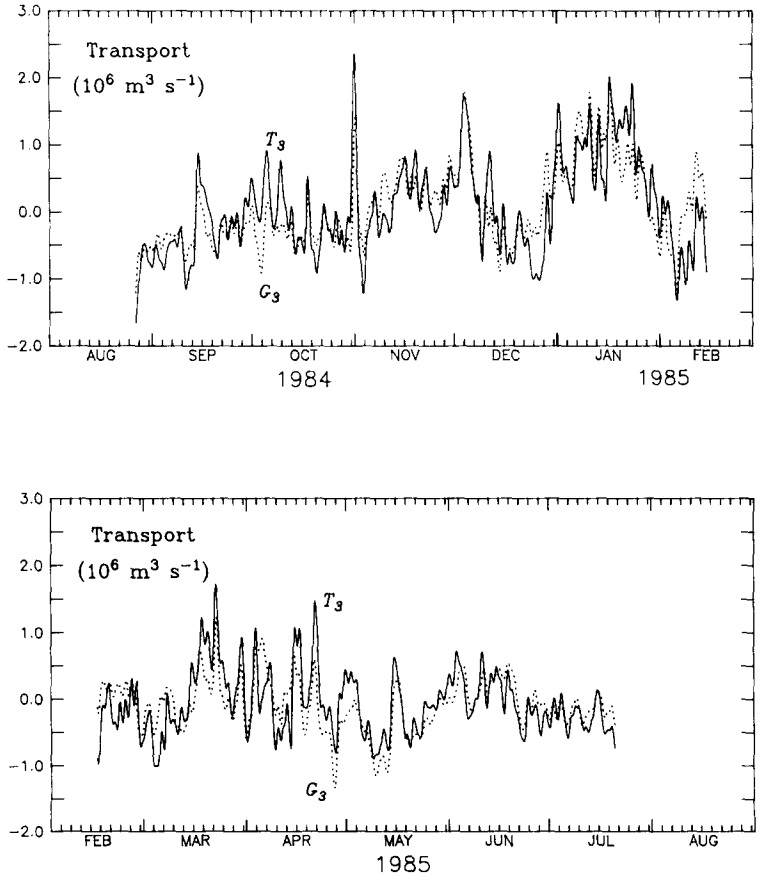

Fig. 7. The demeaned and detrended time series of transport through section 3 from current records (T_3, solid line) and from the bottom pressure records from moorings 7 and 9 (G_3, dotted line).

and outflow events. Except at a period of 10 days, the series were coherent (at the 95% level) and the phase did not differ significantly from zero. The relationship between bottom pressure difference and transport at section 2 was similar to the results at section 3.

CONCLUSIONS

For the first time, estimates of volume transport in the ACC are available from both moored current and bottom pressure records. Our field observations from the Shelikof sea valley and adjacent shelf region between August 1984 and July 1985 lead to the following conclusions:

1. The mean volume transport of the ACC calculated from current records was 0.85×10^6 m^3 s^{-1}. This is in good agreement with estimates of transport from CTD data (provided that the level of no motion is carefully selected to approximate the two-layered velocity field generally present over the sea valley). Approximately 75% of the mean transport was through the sea valley with the remaining flux along the Alaska Peninsula. There was a relative volume transport maximum ($>1.0 \times 10^6$ m^3 s^{-1}) associated with accumulation of freshwater in autumn. The greatest monthly transports, however, occurred in winter and were associated with wind-driven perturbations.
2. Wind forcing was the primary cause of fluctuations in transport. This occurred through Ekman convergence, Ekman pumping (resulting from the curl of the wind stress), and the convergence of transport through Shelikof Strait with that over the open shelf. From estimates of coherence, about half of the transport fluctuations in the ACC were accounted for by the alongshore wind.
3. At sections 2 and 3, transport fluctuations were generally geostrophic. Geostrophy accounted for about 62% of the variance of transport at section 3 and 50% at section 2. While neglecting the terms that are a function of density seemed of little consequence at sections 2 and 3, estimates of geostrophic transport from bottom pressure across section 1 may require time series of density.

The new results further document the relatively vigorous nature of the ACC. Mean transport here is similar in magnitude and more consistent in direction than the northward flux through Bering Strait (MUENCH *et al.*, 1988; COACHMAN and AAGAARD, 1988). Volume transport in the ACC is also greater than observed values for the east coast of North America. Estimates of transport along the shelf of Nova Scotia indicate an annual mean flux of about 0.25×10^6 m^3 s^{-1} which is related to outflow from the Gulf of St. Lawrence (DRINKWATER *et al.*, 1979). Farther south along the coast at Nantucket Shoals, estimates of annual mean volume transport were approximately 0.35×10^6 m^3 s^{-1} (RAMP *et al.*, 1988). Santa Barbara channel (off the west coast of North America) is a region with similar topography to Shelikof Strait; however, forcing for circulation here is oceanic rather than regional runoff. Estimates of transport calculated from current data (BRINK and MUENCH, 1986) for a 2-month period indicate a mean volume flux similar to those during winter in the ACC. Clearly, the ACC is one of the largest and most consistent nearshore currents found along the North American coast.

Acknowledgements—We wish to thank the many people who assisted in field operations, data processing and discussions. In particular we thank the complements of the NOAA ships *Fairweather* and *Discoverer* and the USCG ship *Firebush*. Special thanks to T. Jackson and W. Parker who prepared all the equipment and deployed and recovered the moorings. L. Long and P. Proctor processed the time series with great care and patience. Discussions with R. Reed, L. Incze and R. Romea were extremely useful. Reviewers comments improved the manuscript. This publication is contribution 0071 to the Fisheries Oceanography Coordinated Investigations (FOCI) of NOAA. Contribution no. 984 from Pacific Marine Environmental Laboratory.

REFERENCES

BRINK K. H. and R. D. MUENCH (1986) Circulation in the Pt. Conception–Santa Barbara channel region. *Journal of Geophysical Research*, **91**, 877–895.

BROWN W. S., J. IRISH and C. D. WINANT (1987) A description of subtidal pressure field observations on the northern California continental shelf during the Coastal Ocean Dynamics Experiment. *Journal of Geophysical Research*, **92**, 1605–1636.

COACHMAN L. K. and K. AAGAARD (1988) Transports through Bering Strait: Annual and interannual variability. *Journal of Geophysical Research*, **93**, 15,535–15,539.

DRINKWATER K., B. PETRIE and W. H. SUTCLIFFE. Jr (1979) Seasonable geostrophic volume transports along the Scotian Shelf. *Estuarine and Coastal Marine Science*, **9**, 17–27.

MACKLIN S. A., J. E. OVERLAND and J. P. WALKER (1984) Low-level gap winds in Shelikof Strait. Third Conference on Meteorology of the Coastal Zone, AMS, Boston, Mass., pp. 97–102.

MARINER'S WEATHER LOG (1985) Principal tracks of centers of cyclones at sea level. *Mariners Weather Log*, **29**, 181–182.

MUENCH R. D., J. D. SCHUMACHER and S. A. SALO (1988) Winter currents and hydrographic conditions on the northern central Bering Sea shelf. *Journal of Geophysical Research*, **93**, 516–526.

MYSAK L., R. D. MUENCH and J. D. SCHUMACHER (1981) Baroclinic instability in a downstream varying channel: Shelikof Strait, Alaska. *Journal of Physical Oceanography*, **11**, 950–969.

RAMP S. R., W. S. BROWN and R. C. BEARDSLEY (1988) The Nantucket Shoals Flux Experiment 3. The alongshore transport of volume, heat, salt and nitrogen. *Journal of Geophysical Research*, **93**, 14,039–14,054.

REED R. K. and J. D. SCHUMACHER (1981) Sea level variations in relation to coastal flow around the Gulf of Alaska. *Journal of Geophysical Research*, **86**, 6543–6546.

REED R. K. and J. D. SCHUMACHER (1989) On transport and physical properties in central Shelikof Strait, Alaska. *Continental Shelf Research*, **9**, 261–268.

REED R. K., J. D. SCHUMACHER and L. S. INCZE (1987) Circulation in Shelikof Strait, Alaska. *Journal of Physical Oceanography*, **17**, 1546–1554.

ROACH A. T., J. D. SCHUMACHER and P. STABENO (1987) Observations of currents, surface wind and bottom pressure in Shelikof Strait, Alaska, autumn 1984. NOAA Technical Memorandum ERL PMEL-74, 116 pp. (NTIS no. PB88-121736).

ROYER T. C. (1981) Baroclinic transport in the Gulf of Alaska. Part II. Fresh water driven coastal current. *Journal of Marine Research*, **39**, 251–266.

ROYER T. C. (1982) Coastal fresh water discharge in the northeast Pacific. *Journal of Geophysical Research*, **87**, 2017–2021.

SCHUMACHER J. D. and R. K. REED (1980) Coastal flow in the northwest Gulf of Alaska: the Kenai Current. *Journal of Geophysical Research*, **85**, 5580–6688.

SCHUMACHER J. D. and R. K. REED (1986) On the Alaska Coastal Current in the western Gulf of Alaska. *Journal of Geophysical Oceanography*, **91**, 9655–9661.